

Dear Reviewer (se-2022-17),

We appreciate the time and effort you have spent in reviewing this manuscript. The comments and suggestions helped us improve the manuscript significantly. Our point-by-point responses to the comments are shown below.

1. Reviewer's comment: Regarding the 3-D model. The main topic of the manuscript is to investigate the 'present-day' fault slip rates. However, in constructing the numerical model, the authors assume low fault friction coefficient, thus allowing faults slip aseismically or continuously in the seismogenic layer. Such a practice is inconsistent with what we usually think of as interseismic fault deformation, because during the interseismic phase, faults are locked in the seismogenic zone and freely slipping below it. However, in this study, the fault slip rates are due to average velocities over several seismic cycles. Therefore, the authors should consider their model either reflects long-term kinematics or update the model by locking the faults in the seismogenic layer.

Authors' reply:

Thanks for pointing this out.

The modeled velocities in this paper refer to long-term velocities over several seismic cycles. We mistakenly used the word "present-day" in the title of the original manuscript and we have changed it to "contemporary".

2. Reviewer's comment: A relevant issue that promotes me to judge the model assumption is the GPS velocity profiles shown in figure 13 and 15. The modeled velocities behave as steps across faults, and therefore show discrepancies with GPS observations. The velocity steps are related to the model, which allows faults slip continuously in response to the far-field loading they experience.

Authors' reply:

The locking of the seismogenic zone of the fault during the interseismic phase gives rise to elastic strain accumulation effects that cause across-fault velocity gradients to be smooth. However, in this paper, the faults were set with friction coefficients and allowed to slip to simulate long-term slip rates over several seismic cycles. That is, some of the elastic strain that accumulated on the fault during the interseismic phases is released in the form of fault slip. Therefore, it is reasonable for the modeled velocities to have steps across faults (Thatcher et al., 1999; Hergert and Heidbach, 2010).

Many practices have also indicated that the approach used in the model is feasible (Hergert and Heidbach, 2010; Hergert et al., 2011; Li, Hergert, et al., 2021).

3. Reviewer's comment: A subsequent issue based on the modeling results is the seismic hazards assessment. If the faults are slip continuously in the seismogenic zone, how does elastic strain accumulate? I guess the authors might mis-interpreted the fault slip rate and fault locking; because in calculating strain budget on the Jinqianghe-Maomaoshan-Laohushan faults, they used the 3.5-4.1 mm/a long-term slip rate as stress loading rate (actually in their model, the faults are freely slipping in the seismogenic layer); whereas in interpreting the seismic potential on the Maxianshan-Zhuanglanghe faults, they regarded zero slip rate as reflective of locked fault zone. The above practices are contradictory.

Authors' reply:

We believe that whether the seismogenic zone of a fault is locked depends on the time scale we set. It is obviously that the seismogenic zone is locked during the interseismic period observed by GPS. However, the seismogenic zone can also be considered as unlocked on a long-term time scale, especially when the coseismic displacements of multiple earthquakes can completely compensate for the slip deficit accumulated during fault locking periods (Wang, 2021). Actually, the conclusion that large faults have extremely low effective friction coefficients have been recognized by more and more studies over the past two decades (He et al., 2013; Li et al., 2015; Wang, 2021).

In this paper, the modeled velocity of the faults refers to long-term slip rate which means the sum of the interseismic velocity and coseismic displacement over a period of several seismic cycles. The seismogenic zone of the faults are locked during interseismic period, allowing elastic strain to accumulate.

Regarding the “Locked fault zone” on the Maxianshan-Zhuanglanghe faults, we made an inappropriate description due to language problems. Lines 379–383 of the original manuscript have been rephrased as follows.

Note that the slip rate on the junction between the Maxianshan fault and Zhuanglanghe fault is almost zero. It can be inferred that the junction area would accumulate high concentrations of stress under the continuous eastward movement of the Qilian Block. An earthquake will occur when this stress exceeds the strength of the rocks in this segment. Some have suggested that the 1125 Lanzhou M7.0 earthquake occurred in such a tectonic setting (He et al., 1997; Fig. 14c).

4. Reviewer's comment: Another major issue is the block deformation. In the abstract, the author state that the Bayan Har and Qaidam blocks are deforming continuously, whereas the Qilian block is more of block-like. The main evidences for this conclusion come from the interpretation of velocity gradient within blocks (section 4.3). I disagree with such interpretations, because crustal blocks are rotating with reference to their Euler poles, the velocity gradient within blocks are likely caused by the block rotations. Therefore, unless the authors separate the block rotational components, the velocity gradient inside the block is misinterpreted.

Authors' reply:

Thanks for pointing this out. We did ignore the effect of block rotation in the original manuscript, and the Section 4.3 has been revised as follows.

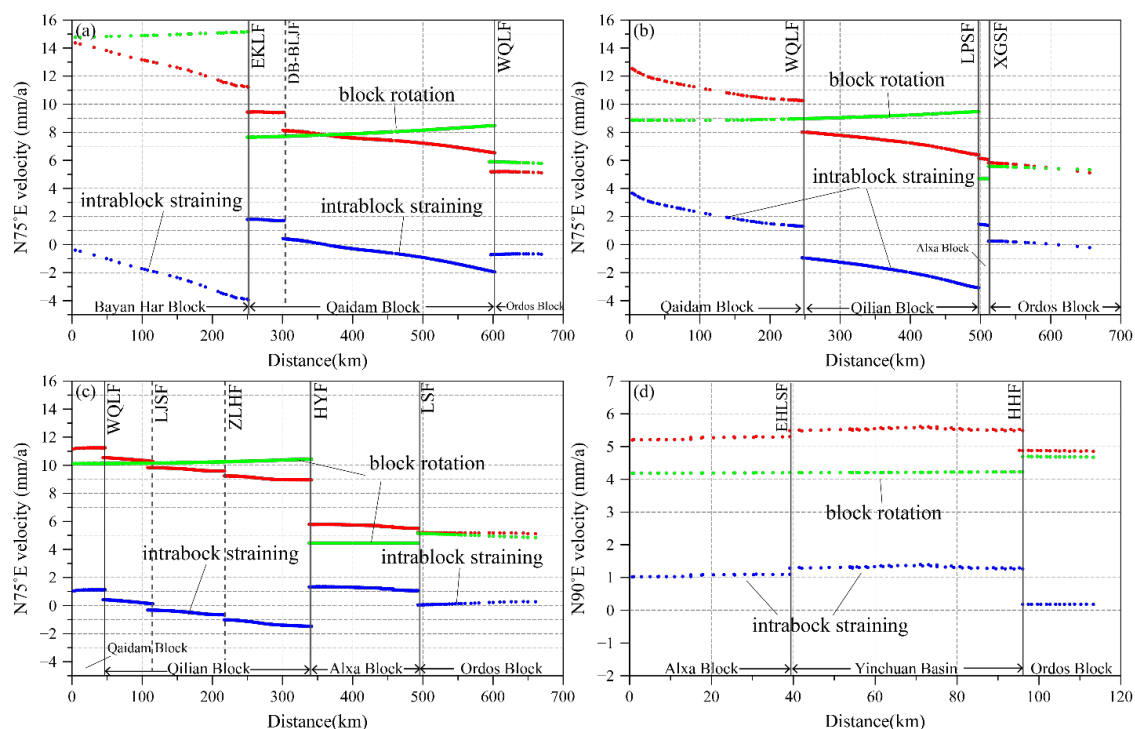


Figure 15. Modeled velocity profiles across the study area with orientation of profiles. The profiles in (a)–(d) correspond to the AA', BB', CC', and DD' in Fig. 12, respectively. The red dots indicate the components along the profiles of the node motion velocity within 2 km on both sides of the profile. The green dots represent the velocity component along the profiles due to plate rotation. The blue dots indicate the differences between the red and green dots. Fault names are defined in Fig. 1.

4.3 Implication for deformation mechanism of NETP

The deformation of NETP is the result of the combined action of block rotation, faulting, and the intra-block straining (Meade and Loveless, 2009). We analyzed four velocity profiles to compare the contributions of block rotation, faulting, and intra-block straining to the total deformation of NETP (Fig. 15). It is noted that the rigid displacements caused by block rotation were calculated according to the Euler pole locations and rotation rates with respect to the Eurasia plate (Wang et al., 2017; Y. Li et al., 2022), as shown in Fig. 15 a–d. The velocity gradient caused by block rotation accounts for more than 80% of that on the profiles. Obviously, the block rotation should

be the primary mechanism for the deformation of the NETP, which is similar to the southeastern Tibet (Z. Zhang et al., 2013). However, the intrablock straining of Bayan Har and Qaidam blocks contribute approximately 4 mm/a and 3 mm/a shortening in profiles of AA', BB' (Fig. 15a–b). The Qilian block also has a contribution of 2 mm/a shortening in profile BB' but decreases to about 1mm/a in profile CC' (Fig. 15b–c). Therefore, the intrablock straining is still significant for regional deformation. The boundary faults of the blocks, such as the East Kunlun fault, Haiyuan fault, West Qinling fault, also play an important role in regulating the deformation differences between blocks.

The D–D' profile shows that the tectonic deformations of the Yinchuan Basin structural belt slightly differ from those in other profiles. The NE expansion of the TP leads to near-N–S compression on the Yinchuan Basin (Yang, 2018), which causes it to move eastwards faster than the Alxa Block. This manifests as an eastward extension in the Yinchuan Basin. The crustal deformations caused by this process are accommodated by the right-lateral strike-slip of Huanghe Fault (Fig. 15d).

5. Reviewer's comment: There are also quite a lot of language and/or grammar issues. I would suggest the authors seek help from native speakers or professional services.

Authors' reply:

Thanks for your suggestion, we have used the services of a professional English editing company to improve the language of the manuscript.

6. Reviewer's comment: Based on my above judgements, I suggest a major revision for the manuscript.

Authors' reply:

Thanks for your valuable comments and suggestions.

We have carefully revised the full text, please pay attention to the revised manuscript.

7. Reviewer's comment: There are also lots of language and/or grammar and other minor issues. I just name a few:

7.1 Reviewer's comment: Line27-28, give references

Authors' reply:

Thanks for your suggestions. We have reorganized the language there and added references as follows.

Having experienced the strong Cenozoic deformation, crust of this area develops a complex fault system with several large and deep faults, such as the generalized Haiyuan fault (F1), West Ordos fault (F2), West Qinling fault (F3), East Kunlun fault (F4), that divide the NETP into the Alxa, Ordos, Qilian, Qaidam, and Bayan Har blocks (Zhang et al., 2003; Fig.1). These faults are characterized by extremely intense tectonic movements and seismic activities (Zhang, 1999; Zheng et al., 2016b).

7.2 Reviewer's comment: Line34, please explicitly indicate the earthquake locations in figure 1.

Authors' reply:

We have labeled all earthquakes greater than magnitude 8 on Fig. 1 as follows.

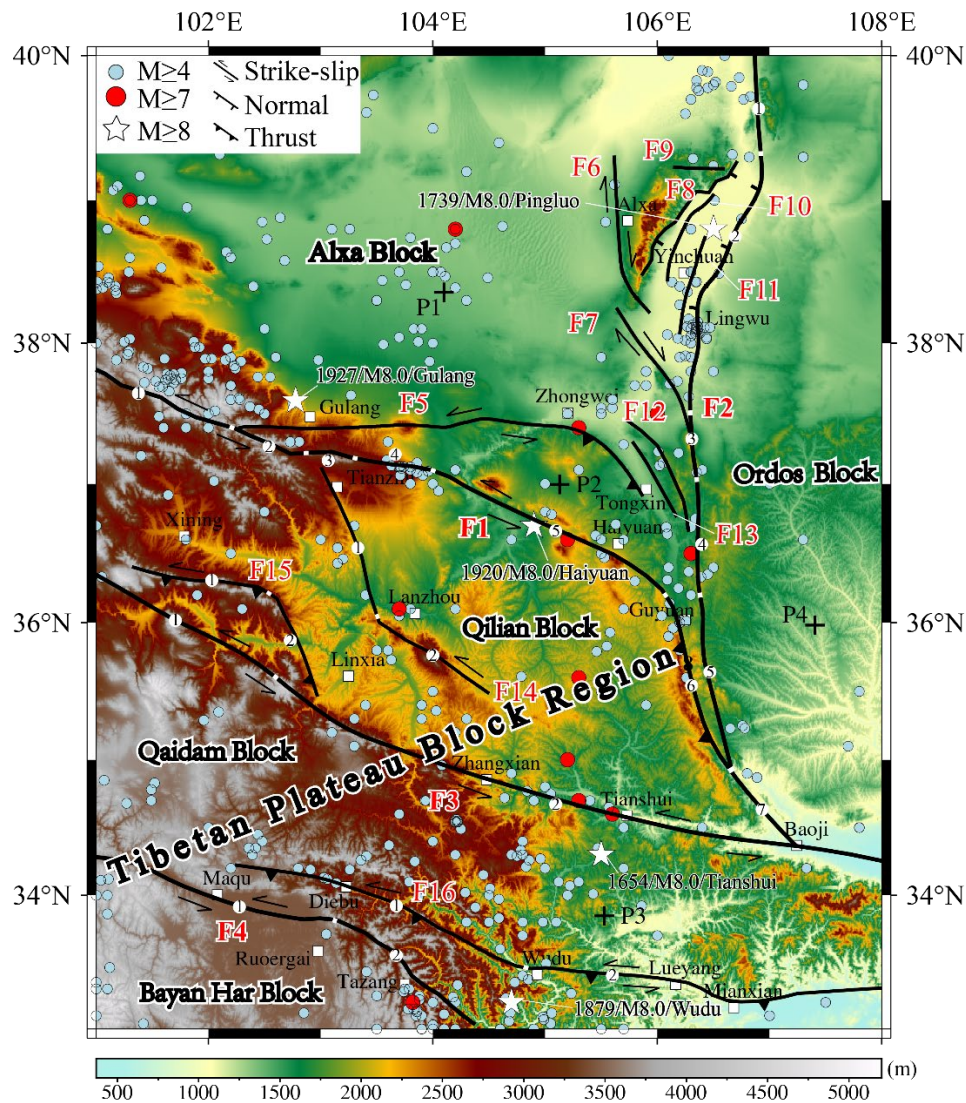


Figure 1. Earthquakes with magnitude $M \geq 8.0$ are labeled.

7.3 Reviewer's comment: Line36, what is the strength of an earthquake?

Authors' reply:

We have rephrased the sentence as follows.

Since the generation and magnitude of an earthquake is closely related to fault activity, long-term fault slip rate plays a key role in medium- and long-term seismic hazard assessment (Ding et al., 1993; Xu et al., 2018).

7.4 Reviewer's comment: Line39, the sentence reads quite strange, rephrase

Authors' reply:

We have rephrased the sentence as follows.

For example, combined with coseismic displacements, long-term fault slip rates can be used to calculate earthquake recurrence interval (Shen et al., 2009) and assess the magnitudes of potential earthquakes (Bai et al., 2018; Hergert and Heidbach, 2010).

7.5 Reviewer's comment: Line48-49, actually, quite a lot previous studies adopted elastic block models (e.g., Y. Li et al., 2017, 2021), and their results show non-negligible internal deformation

Authors' reply:

Thanks for pointing this out. We have rephrased the sentences as follows.

For example, the geological slip rates only represent the activities of one fault branch that measured in a fault zone, which is always consist of several branches. They are usually lower than the geodetic slip rates on the fault as a whole if a rigid block assumption is adopted in the geodetic inversion process (Shen et al., 2009). However, several crustal deformation studies conducted in TP demonstrated that the internal block deformation in the NETP cannot be ignored (Royden et al., 1997; Zhang et al., 2004; Y. Li et al., 2017, 2021).

7.6 Reviewer's comment: Line58, partitioning of deformation modes? What does it mean?

Authors' reply:

In the original manuscript, we intended to analyze whether the deformation pattern of the NETP is a block model or a continuum model according to the distribution characteristics of the velocity gradient. In subsequent manuscript, we will make adjustments to this description as follows.

Based on these results, we summarized the long-term crustal deformation characteristics in the NETP.

7.7 Reviewer's comment: Figure1, indicate the time span of earthquakes and the sources, give descriptions of P1-P3.

Authors' reply:

Thanks for your suggestions. We updated the Figure 1 caption as follows:

Figure 1. Map of active faults and earthquakes of the NETP. Black lines represent the active faults. The light blue, red dots and the white pentagrams represent earthquakes from 1831 BC to 2017 AD from the National Earthquake Data Center (<http://data.earthquake.cn>). Black crosses (P1-P4) indicate the locations of four test sites for the comparison with the numerical model shown in Figure 3b. Faults discussed in the text are labeled as followed.....

7.8 Reviewer's comment: Line84-85, cite references

Authors' reply:

We will add corresponding references. The updated text is shown below.

Lithospheric faults (i.e., F1, F2, F3, and F4) cut through the Moho and reach the bottom of the model (Zhan et al., 2005; B. Liu et al., 2017; Zhao et al., 2015; Fig. 2a, b; Table 1). All other faults are crustal faults that terminate in the upper, middle, or lower crust (Yuan et al., 2002b, 2003; Lease et al., 2012; Meng et al., 2012; B. Liu et al., 2017; Wu et al., 2020).

7.9 Reviewer's comment: Table1, list the references in the table

Authors' reply:

We added a column to the right of the table for references.

Table 1. Geometric parameters of faults in the model

	Fault name	Strike	Dip direction	Dip (°)	Reference
F1	/	NWW-SSE	SW	70	RGAFSAO, 1988
F2-1	ZZSF	N-S	W	70	Gao, 2020
F2-2	HHF	N-S	W	70	Bao et al., 2019
F2-3	LSF	N-S	W	80	Wang et al., 2013
F2-4	YWSF	N-S	W	70	NIGS, 2017
F2-5	XGSF	N-S	W	70	NIGS, 2017
F3-1	DTH-LXF				Zhou et al., 2009
F3-2	WQLF	NWW-SSE	NE	70	Li, 2005
F4-1	EKLF	NW-SE	NE	75	Z. Liu et al., 2017
F4-2	TZF				J. Li et al., 2019
	East TJSF	NW-SE	SW	70	RGAFSAO, 1988
F5	West TJSF	E-W	S	70	RGAFSAO, 1988
F6	WHLSF	N-S	W	80	Lei, 2015
F7	NSSF	NW-SE	SW	70	RGAFSAO, 1988
F8	EHLSF	NE-SW	SE	60	Du, 2010
F9	ZYGF	E-W	S	60	NIGS, 2017
F10	LHTF	NNE-SSW	SE	70	NIGS, 2017
F11	YCF	NNE-SSW	NW	70	NIGS, 2017
F12	YTSTF	NW-SE	SW	65	NIGS, 2017
F13	QSHF	NW-SE	SW	45	Tian et al., 2020
F14-1	ZLHF	NNW-SSE	SW	45	Xu et al., 2016
F14-2	MXSF	NW-SE	SW	80	Hou et al., 1999
F15	LJSF	NWW-SSE	SW	50	Yuan et al., 2005
F16-1	DB-BLJF	NW-SE	SW	70	Yuan et al., 2007
F16-2	WD-KXF	E-W	SW	70	Jia et al., 2012

The detailed fault names are defined in Fig. 1.

7.10 Reviewer’s comment: Line125, change critically important to important

Authors’ reply:

Thanks for your suggestion. We have changed it.

7.11 Reviewer’s comment: Line134, fitting misfit in mm/a or cm/a or others?

Authors’ reply:

The *misfit* is a dimensionless unit. It was calculated as follows (Cianetti et al., 2001):

$$misfit = \frac{\sum_i |\vec{V}_{GPS} - \vec{V}_{mod}|}{\sum_i |\vec{V}_{GPS}| + \sum_i |\vec{V}_{mod}|}$$

7.12 Reviewer’s comment: Line135, I am not fully understood, why F2 and F3 are not considered in friction coefficients adjustments?

Authors’ reply:

I guess you probably meant to refer to F2 and F4?

Actually, F1–F4 were all considered in the numerical simulation tests of friction coefficients adjustments. However, the adjustment of friction coefficients of F2 and F4 did little help to reduce the misfit value. Therefore, the friction coefficients of F2 and F4 remained unchanged.

7.13 Reviewer’s comment: Line136, it seems to me, for F3, friction coefficient from 0.02 to 0.1 is large, why?

Authors’ reply:

Let’s first correct a mistake in the *misfit* calculation in Figure 3a of the original manuscript. Due to a coding error, the calculation of *misfit* in the original manuscript only considers the easting components of the GPS observations and modeled velocities. Now we have corrected the error and the updated Fig. 3a is shown in Fig. R2. The value of 0.02 can still be considered as the best friction coefficient.

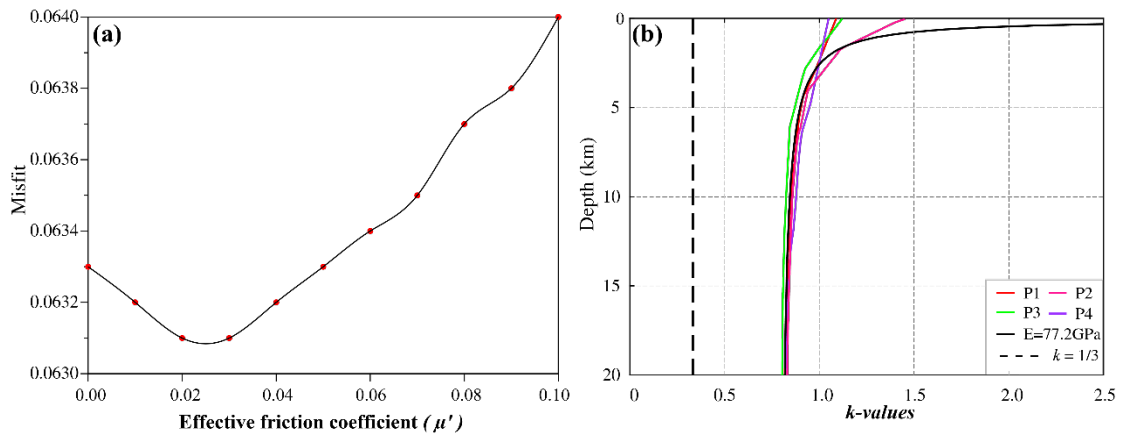


Figure 3. A friction coefficient of 0.02 or 0.03 for all faults yields the smallest fitting error.

Now let’s answer your question about “Line136, it seems to me, for F3, friction coefficient from 0.02 to 0.1 is large, why”.

We determined this value through multiple numerical simulation tests. We found that increasing the friction coefficient of F3 and decreasing the friction coefficient of F1 is beneficial to the reduction of misfit. The simulation tests are as follows (Table R1). The misfit value is the lowest when the friction coefficients of F1 and F3 are 0.01 and 0.1, respectively.

Table R1. The simulation tests to find the lowest misfit

μ'	F3=0.04	F3=0.05	F3=0.06	F3=0.07
<i>misfit</i>	0.6078	0.05965	0.05855	0.05749
μ'	F3=0.07; F1=0.01	F3=0.08; F1=0.01	F3=0.09; F1=0.01	F3=0.10; F1=0.01
<i>misfit</i>	0.05639	0.05542	0.05449	0.05362

7.14 Reviewer's comment: Line163, Wang et al. (2020) should be Wang and Shen (2020), check the whole manuscript to avoid similar mistakes.

Authors' reply:

Thanks for pointing this out. We have corrected all similar mistakes.

7.15 Reviewer's comment: Line180, see the 5th major comment. I don't agree with this interpretation, velocity gradient within blocks might be related to block rotation as well!

Authors' reply:

Thanks for pointing this out. We have removed the relevant text.

7.16 Reviewer's comment: Line187, crustal velocity, not crust speed. Check and replace the whole manuscript

Authors' reply:

Thanks for pointing this out. We have checked the whole manuscript and made changes.

7.17 Reviewer's comment: Line215, older?

Authors' reply:

Thanks for pointing this out. We have replaced it with "earlier".

7.18 Reviewer's comment: Line215-217, give reasons for the discrepancies

Authors' reply:

We believe that there are two reasons for this.

First, early studies were based on geological methods with larger time scale. Second, the slip rate of the fault could not be better constrained in the past due to limited data (Li, et al., 2009).

We have already added it to the updated manuscript.

7.19 Reviewer's comment: Table3, change table to figure, which shows 1:1 plots of fault slip rates

Authors' reply:

Thanks for your suggestion.

We have carefully considered this issue, referring to the Figure 3 in the paper of Y. Li et al. (2021). The difference between the results obtained by the two methods can be clearly intuitively observed from the figure.

However, the modeled slip rates vary with the locations of the faults in this paper. It is also inappropriate to use a mean value to replace the slip rate of the entire fault. Therefore, we retained the Table3 used in the original manuscript.

7.20 Reviewer's comment: Line297, rephrase the sentence

Authors' reply:

Thanks for your suggestion. We have rephased the sentence as follows.

In order to further examine the fit between the model results and GPS data, we selected a NE–SW profile that crosses through the study area (Fig. 12, C–C') and projected all GPS-observed values within 50 km of both sides of the profile.

7.21 Reviewer's comment: Line300, see the 1st and 2nd major comments. It seems to me that the differences are large, especially across faults. The modeled velocities have steps across faults, this should be result from the fact that numerical model does not consider fault locking

Authors' reply:

It has been explained before.

Please see the replies to comment 2 and 3.

7.22 Reviewer's comment: Line315-319, I don't think the way of earthquake potential assessment appropriate. First, aseismic creep is not found along the Jinqianghe and Maomaoshan faults, as recent studies show. Second, the seismogenic does not corresponds to 20 km. Check the latest studies (e.g., Y. Li, 2021, JGR) to update your way of calculation.

Authors' reply:

Thanks for pointing this out.

The aseismic creep rates have been updated according to the latest study (Y. Li, et al., 2021). We also learned that the locking depth of the Laohushan fault or the Tianzhu Seismic Gap is about 20–22 km according to Y. Li et al. (2017, 2021), which is approximately equal to the data used in our manuscript. The new calculation results are shown in the table below.

Table 4 Earthquake magnitude and recurrence interval of each fault based on the energy accumulated during the elapsed time since the last remarkable earthquake

Fault name	V_1 (mm/a)	V_2 (mm/a)	L_1 (km)	L_2 (km)	μ (Gpa)	t	S (m)	M_S	T (a)
JQHF	3.5	/	34	20	34.5	675	1.5	7.1	424
MMSF	3.9	/	51	20	34.5	952	2.2	7.3	571
LHSF	4.1	2.5	70	20	34.5	133	3.1	6.6	1910
MSLPSF, SSLPSF	2.5	/	80	23	34.5	570	3.5	7.2	1397
GG-BJF	0.7	/	70	23	34.5	1400	3.1	7.1	4365

V_1 is the modeled average slip rate of the fault in this study; V_2 is the aseismic creep rate of the fault (Y. Li, et al., 2021); L_1 is the length of the fault (Xu et al., 2016); L_2 is the depth of the seismogenic, which refers to the locking depth (Y. Li, et al., 2017, 2021); μ is the shear modulus of the rocks (Aki et al., 2002); t is the time that has elapsed since the most recent remarkable earthquake (Gan et al., 2002; Shi et al., 2013, 2014; Wang et al., 2001); S is the largest maximum coseismic displacement, calculated using the method of Gan et al. (2002); M_S is the earthquake magnitude corresponding to the energy accumulated by the fault between recurrences (Purcaru et al., 1978); T is the recurrence interval of the earthquake, where $T = S/(V_1 - V_2)$ (Shen et al., 2009). The fault names are defined in Fig. 1 and Fig. 14.

References (only new)

- Bao G., Chen H., Hu J., and Zhu G.: Quaternary Activity and Segmentation of the Yellow River Fault of the Eastern Margin of Yinchuan Graben, *Acta Geoscientica Sinica*, 40, 614–628, 2019.
- Du P.: Studying on the active characteristics and paleoearthquake of the eastern piedmont fault of Helan Mountain in the late Quaternary, M.S. thesis, China University of Geosciences (Beijing), Beijing, 2010.
- Gao Z.: Late Quaternary activity characteristics and risk analysis of large earthquakes of the Zhuozishan West Piedmont Fault, M.S. thesis, Lanzhou Institute of Seismology, China Earthquake Administration, Lanzhou, 2020.
- Jia W., Liu H., Liu Y., and Yuan D.: Preliminary study on activity of the Wudu-Kangxian fault zone, *Northwestern Seismological Journal*, 34, 142–149, 2012.
- Lease R. O., Burbank D. W., Zhang H., Liu J., and Yuan D.: Cenozoic shortening budget for the northeastern edge of the Tibetan Plateau: Is lower crustal flow necessary? , *Tectonics*, 31, TC3011, <https://doi.org/10.1029/2011TC003066>, 2012.
- Lei J.: Research on activity of the West Helanshan fault, M.S. thesis, The Institute of Crustal Dynamics, China Earthquake Administration, Beijing, 2015.

- Li C.: Quantitative studies on major active fault zones in Northeastern Qinghai-Tibet Plateau, PH.D. thesis, Institute of Geology, China Earthquake Administration, Beijing, 2005.
- Li J., Cai Y., and Zhang J.: Geometric structure and slip gradient model of the Tazang fault in the east Kunlun fault zone, *Earthquake*, 39, 20–28, 2019.
- Li Y., Nocquet J. M., Shan X., and Song X.: Geodetic observations of shallow creep on the Laohushan-Haiyuan Fault, Northeastern Tibet, *J. Geophys. Res. Sol. Ea.*, 126, <https://doi.org/10.1029/2020JB021576>, 2021.
- Li Y., Nocquet J. M., and Shan X.: Crustal deformation across the western Altyn Tagh fault (86° E) from GPS and InSAR, *Geophys. J. Int.*, 228, 1361–1372, <https://doi.org/10.1093/gji/ggab403>, 2022.
- Liu B., Feng S., Ji J., Wang S., Zhang J., Yuan H., and Yang G.: Lithospheric structure and faulting characteristics of the Helan Mountains and Yinchuan Basin: Results of deep seismic reflection profiling, *Sci. China Earth Sci.*, 60, 589–601, <https://doi.org/10.1007/s11430-016-5069-4>, 2017.
- Liu Z., Tian X., Gao R., Wang G., Wu Z., Zhou B., Tan P., Nie S., Yu G., Zhu G., and Xu X.: New images of the crustal structure beneath eastern Tibet from a high-density seismic array, *Earth Planet Sc. Lett.*, 480, 33–41, <https://doi.org/10.1016/j.epsl.2017.09.048>, 2017.
- Meade B. J., and Loveless J. P.: Block modeling with connected fault-network geometries and a linear elastic coupling estimator in spherical coordinates, *B. Seismol. Soc. Am.*, 99, 3124–3139, <https://doi.org/10.1785/0120090088>, 2009.
- Meng X., Shi L., Guo L., Tong T., and Zhang S.: Multi-scale analyses of transverse structures based on gravity anomalies in the northeastern margin of the Tibetan Plateau, *Chinese J. Geophys.*, <https://doi.org/10.6038/j.issn.0001-5733.2012.12.006>, 2012.
- Ningxia Institute of Geological Survey (NIGS): Regional geology of Ningxia Hui Autonomous Region, Geological Publishing House, Beijing, 2017.
- The Research Group on Active Fault Systems around the Ordos Massif (RGAFSAO): Active fault system around Ordos Massif, Seismological Press, Beijing, 1988
- Thatcher W., Foulger G. R., Julian B. R., Svarc J., Quilty E., and Bawden G. W.: Present-Day deformation across the basin and range province, western united states, *Science*, 283, 1714–1718, <https://doi.org/10.1126/science.283.5408.1714>, 1999.
- Tian J., Li M., Liang Z., Li L., Yan G., Lu M., and Tan Z.: Tectonic evolution of the Qingshuihe Basin since the Late Miocene: Relationship with north-eastward expansion of the Tibetan Plateau, *Geol. J.*, 55, 7148–7166, <https://doi.org/10.1002/gj.3650>, 2020.
- Wang K.: On the strength of subduction megathrusts, *Chinese J. Geophys.*, 64, 3452–3465, <https://doi.org/10.6038/cjg2021P0515>, 2021.
- Wang W., Qiao X., Yang S., and Wang D.: Present-day velocity field and block kinematics of Tibetan Plateau from GPS measurements, *Geophys. J. Int.*, 208, 1088–1102, <https://doi.org/10.1093/gji/ggw445>, 2017.
- Wang W., Zhang P., and Lei Q.: Deformational characteristics of the Niushoushan-Luoshan fault zone and its tectonic implications, *Seismology and Geology*, 35, 195–207, <https://doi.org/10.3969/j.issn.0253-4967.2013.02.001>, 2013.
- Wu G., Tan H., Sun K., Wang J., Xi Y., and Shen C.: Characteristics and tectonic significance of gravity anomalies in the Helanshan-Yinchuan Graben and adjacent areas, *Chinese J. Geophys.*, 63, 1002–1013, <https://doi.org/10.6038/cjg2020N0233>, 2020.

- Yuan D., Liu B., Zhang P., Liu X., Cai S., and Liu X.: The neotectonic deformation and earthquake activity in Zhuanglang river active fault zone of Lanzhou, *Acta Seismologica Sinica*, 24, 441–444, 2002b.
- Yuan D., Zhang P., Lei Z., Liu B., and Liu X.: A preliminary study on the new activity features of the Lajishan mountain fault zone in Qinghai province, *Earthquake Research in China*, 21, 93–102, 2005.
- Yuan D., Lei Z., He W., Xiong Z., Ge W., Liu X., and Liu B.: Textual research of Wudu earthquake in 186 B.C. in Gansu Province, China and discussion on its causative structure, *Acta Seismologica Sinica*, 20, 696–707, 2007.
- Zhan Y., Zhao G., Wang J., Tang J., Chen X., Deng Q., Xuan F., and Zhao J.: Crustal electric structure of Haiyuan arcuate tectonic region in the northeastern margin of Qinghai-Xizang Plateau, China. *Acta Seismologica Sinica*, 27, 431–440, 2005.
- Zhao L., Zhan Y., Chen X., Yang H., and Jiang F.: Deep electrical structure of the central West Qinling orogenic belt and blocks on its either side, *Chinese J. Geophys.*, 58, 2460–2472, <https://doi.org/10.6038/cjg20150722>, 2015.
- Zhang Z., McCaffrey R., and Zhang P.: Relative motion across the eastern Tibetan plateau: Contributions from faulting, internal strain and rotation rates, *Tectonophysics*, 584, 240–256, <http://doi.org/10.1016/j.tecto.2012.08.006>, 2013.
- Zheng W., Yuan D., Zhang P., Yu J., Lei Q., Wang W., Zheng D., Zhang H., Li X., Li C., and Liu X.: Tectonic geometry and kinematic dissipation of the active faults in the northeastern Tibetan Plateau and their implications for understanding northeastward growth of the plateau, *Quaternary Sciences*, 36, 775–788, <https://doi.org/10.11928/j.issn.1001-7410.2016.04.01>, 2016b.
- Zhou B., Peng J., and Zhang J.: Development and distribution patterns of active fault zones in Qinghai province, *Journal of Engineering Geology*, 17, 612–618, 2009.